IEEE Access
Multidisciplinary | Rapid Review | Open Access Journal

SPECIAL SECTION ON ADVANCED ENERGY STORAGE TECHNOLOGIES AND THEIR APPLICATIONS

Received August 9, 2018, accepted September 19, 2018, date of publication October 1, 2018, date of current version March 8, 2019.

Digital Object Identifier 10.1109/ACCESS.2018.2872792

Accelerated Adaptive Second Order Super-Twisting Sliding Mode Observer

CHENG LIN[1], SHENGXIONG SUN[1,2], PAUL WALKER[2], AND NONG ZHANG[2]
[1]National Engineering Laboratory for Electric Vehicles, Beijing Institute of Technology, Beijing 100081, China
[2]Faculty of Engineering and Information Technology, University of Technology Sydney, Ultimo, NSW 2007, Australia

Corresponding author: Shengxiong Sun (shengxiong.sun@student.uts.edu.au)

This work was supported in part by the National Natural Science Foundation of China under Grant 51575044 and in part by the National Key R&D Program of China under Grant 2017YFB0103801.

ABSTRACT An accelerated second-order super-twisting sliding mode observer with an adaptive gain is proposed for a typical nonlinear system. The key contribution of this algorithm is that the rate of convergence of observation error is accelerated remarkably by introducing "system damping." Chattering issue is attenuated with a satisfactory performance compared with conventional sliding mode observer. Furthermore, adaptive gain can vary with deviation between the trajectory and the sliding mode switching manifold dynamically so that overshoot can be reduced. The novel observer is proven mathematically to be convergent in a finite time. Finally, an example of nonlinear system is given to verify the performance.

INDEX TERMS Sliding mode, accelerated, super-twisting, observer.

I. INTRODUCTION

Since sliding mode controllers (SMC) have been applied for several decades, they are regarded as effective ways to control a wide spectrum of perturbed nonlinear systems with good robustness [1], [2]. SMC is still considered as one of the best choices in various engineering practices up to now [3]–[5]. Based on the same concept, different sorts of sliding mode observers (SMO) have been developed to robustly estimate the system states. These are widely used in sensorless operation conditions so that costs will be reduced [6]–[10]. However, the main defect of sliding mode algorithms is the chattering issue that resulted from the existence of the discontinuous switch function. It is inherent and cannot be eliminated absolutely but it can be attenuated. Currently there are three typical methods to reduce chattering as follows [11]: (i) substituting "saturation" or "sigmoid function" or "inverse tangent function" for the discontinuous sign function [12]. It is the simplest and the most widely used way to reduce chattering, it is omitted here because of its familiarity. In order to emphasize performance of algorithm, sign function is kept in this article. (ii) Using high order sliding mode (HOSM) observers [13], [14]. It has been applied to practice successfully such as PEM fuel cell system [15], [16] and estimation of tire friction [17]. However, the generalization of rth-order ($r \geq 3$) sliding mode observer is limited by high relative degree issues, consecutive derivatives of the variable ($s, \dot{s}, \ddot{s}, \cdots s^{(n-1)}$) must be known. It is worth noting that, as one of the most powerful second-order sliding mode observers, super-twisting (STW) only needs information of the sliding variable s [18], [19], it can generate a continuous function to drive the sliding variables and derivatives of sliding variables to 0 in a finite time and it shows a good robust performance without knowing the boundary of disturbance exactly [20]. Based on the twisting controller, Dvir and Levant [21] proposed a modified twisting controller for uncertain dynamic systems with relative degree 2, the convergence rate is prescribed in advance and the twisting control algorithm can be accelerated. (iii) Introducing an adaptive gain [11], [22], [23]. The variable gain will vary with distance between the trajectory and sliding mode switching manifold, if deviation is larger than a certain range, the adaptive gain will be increasing to force the trajectory back to sliding mode switching manifold and if deviation is small, the adaptive gain will reduce to prevent the system from overshoot. This can attenuate chattering and compensate perturbations of which boundaries are time-variant more accurately [24]. The adaptive super-twisting (ASTW) algorithm has been applied in sensorless control for permanent magnet synchronous motor with good performance [25].

The main objective of this article is to propose an accelerated adaptive second order super-twisting sliding mode observer (AASTW) based on previous distinguished achievements of sliding mode algorithms. By introducing "system damping", a concept proposed by Slotine in 1986 [26],

the rate of convergence of observation error is further increased in a finite time, so that performance of the sliding mode observer is further enhanced.

II. PROBLEM STATEMENT

In this paper, the following nonlinear system with bounded parameters and disturbance is considered:

$$x^{(n)}(t) = f(t, \mathbf{x}, u) + \delta(t, \mathbf{x}, u), \quad \mathbf{x} = \left[x, \dot{x}, \ddot{x}, \cdots x^{(n-1)}\right]^{\mathrm{T}} \tag{1}$$

It can be transformed into a corresponding equation of state in (2), where y is the output of the system and x_1 can be measured directly, $u(t)$ is the input of the observer, δ is disturbance. Let $\hat{\mathbf{x}}$ indicate the state estimation, $\tilde{\mathbf{x}}$ indicate the estimation error, $\tilde{\mathbf{x}} = \mathbf{x} - \hat{\mathbf{x}}$.

$$\begin{cases} \dot{x}_1 = x_2 \\ \dot{x}_2 = x_3 \\ \vdots \\ \dot{x}_n = f(t, \mathbf{x}, u) + \delta(t, \mathbf{x}, u) \\ y = x_1 \end{cases} \tag{2}$$

Assumption 1: The system $f(t, \mathbf{x}, u)$ in (2) is a continuous function that is not known with high accuracy, but its uncertainty $\xi(t, \mathbf{x}, u)$ is bounded by Ξ, $\Xi \geq 0$, it can be expressed with model function $\hat{f}(t, \mathbf{x}, u)$ as $f(t, \mathbf{x}, u) = \hat{f}(t, \mathbf{x}, u) + \xi(t, \mathbf{x}, u)$, where $|\xi(t, \mathbf{x}, u)| \leq \Xi$.

Assumption 2: The disturbance δ is bounded, $|\delta| \leq \Delta$, $\Delta \geq 0$.

Remark 1: The essence of applying accelerated adaptive super-twisting sliding observer to system (1) is forcing the observed vector $\hat{\mathbf{x}}$ to track the expected vector $\mathbf{x}$ faster, so that it drives estimation errors $\tilde{\mathbf{x}} \to \mathbf{0}$.

III. OBSERVER DESIGN

A second order nonlinear system is taken into consideration, this can be generalized to the systems containing more elements in vectors $\mathbf{x_1}$ and $\mathbf{x_2}$ based on the same principle. The proposed accelerated adaptive super-twisting sliding mode observer has the form shown in (3).

$$\begin{cases} \dot{\hat{x}}_1 = \alpha_1 \left(x_1 - \hat{x}_1\right) + \hat{x}_2 + k_1 \left|x_1 - \hat{x}_1\right|^{1/2} \operatorname{sgn}\left(x_1 - \hat{x}_1\right) \\ \dot{\hat{x}}_2 = \alpha_2 \left(x_1 - \hat{x}_1\right) + \hat{f}\left(t, x_1, \hat{x}_2, u\right) + k_2 \operatorname{sgn}\left(x_1 - \hat{x}_1\right) \end{cases} \tag{3}$$

and its corresponding estimation errors equations of state in (4)

$$\begin{cases} \dot{\tilde{x}}_1 = -\alpha_1 \tilde{x}_1 + \tilde{x}_2 - k_1 \left|\tilde{x}_1\right|^{1/2} \operatorname{sgn}(\tilde{x}_1) \\ \dot{\tilde{x}}_2 = -\alpha_2 \tilde{x}_1 + f\left(t, x_1, \hat{x}_2, u\right) - \hat{f}\left(t, x_1, \hat{x}_2, u\right) \\ \qquad + \delta(t, x_1, x_2, u) - k_2 \operatorname{sgn}(\tilde{x}_1) \end{cases} \tag{4}$$

where $\alpha_{1,2}$ is positive constant value, and the $\alpha\tilde{x}$ is so called "system damping", the k_1 and k_2 are adaptive gains defined as

$$\dot{k}_{1,2} = \begin{cases} \lambda_{1,2} \operatorname{sgn}\left(\left|x_1 - \hat{x}_1\right| - \mu_{1,2}\right) & \text{if } k_{1,2} > \kappa_{1,2} \\ 0 & \text{if } k_{1,2} \leq \kappa_{1,2} \end{cases} \tag{5}$$

where $\lambda_{1,2}$, $\mu_{1,2}$, κ are constant values, but κ cannot be a small arbitrarily value and it should be selected according to the limit of $k_{1,2}$ which will be discussed in the following text.

Remark 2: μ in (5) plays a role as a detector, when the estimation error $\tilde{x}_1$ comes through the limit $|\tilde{x}_1| \leq \mu$, the adaptive gains will reduce dynamically and start a fine tuning phase, so that overshoot of the trajectory can be further weakened until it leaves this domain as illustrated in Fig. 1.

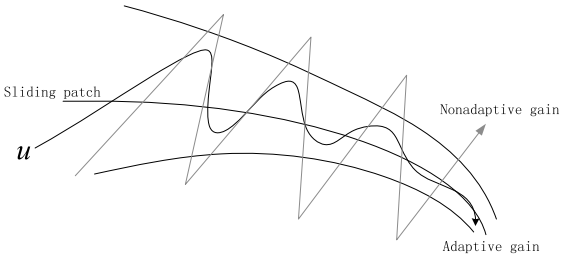

FIGURE 1. Sketch map of adaptive gain effect.

Lemma: The adaptive gains k_1 and k_2 in (5) are bounded.

Proof: (i) If $k_{1,2}$ comes into the interval $k_{1,2} \leq \kappa_{1,2}$, it is a constant value. (ii) If $k_{1,2}$ is in the interval $k_{1,2} > \kappa_{1,2}$, integrate both sides of (5) and obtain the solution of the differential equation

$$k_{1,2} = k(t_0) \pm \lambda_{1,2} \cdot t, \quad t \in \left[t_0, t_f\right] \tag{6}$$

Therefore, in a finite time domain $k_{1,2}$ is bounded, the Lemma is proven.

Theorem 1: Based on Assumption 1 and Assumption 2, the proposed observer in (3) and (4) for nonlinear systems in (1) can drive the estimation errors $(\tilde{x}_1, \tilde{x}_2) \to (0, 0)$.

Proof: All kinds of observers are always affected by noise or disturbance in engineering practice, so robustness plays a critical role in the performance of the observer, this proof is based on Davila *et al.*'s proof method [27] and noise or disturbance is taken into consideration. Let $F\left(x_1, x_2, \hat{x}_2\right) = f(t, x_1, x_2, u) - \hat{f}\left(t, x_1, \hat{x}_2, u\right) + \delta(t, x_1, x_2, u)$.

It is bounded according to Assumption 1 and Assumption 2, there exists a constant F_0, $F_0 \geq 0$, such that $\left|F\left(x_1, x_2, \hat{x}_2\right)\right| \leq F_0$, (4) can be transformed into

$$\begin{cases} \dot{\tilde{x}}_1 = -\alpha_1 \tilde{x}_1 + \tilde{x}_2 - k_1 \left|\tilde{x}_1\right|^{1/2} \operatorname{sgn}(\tilde{x}_1) \\ \dot{\tilde{x}}_2 = -\alpha_2 \tilde{x}_1 + F\left(x_1, x_2, \hat{x}_2\right) - k_2 \operatorname{sgn}(\tilde{x}_1) \end{cases} \tag{7}$$

$k_{1,2}$ is adaptive as shown in (5) on the premise that it satisfies the following inequalities.

$$\begin{cases} k_1 > [2/(k_2 - F_0)]^{(1/2)} (k_2 + F_0 + \Lambda)(1 + p)/(1 - p) \\ k_2 > F_0 \end{cases} \tag{8}$$

where p is a constant value, $p \in (0,1)$, $\Lambda \geq \alpha_2 \tilde{x}_{1\max}^2$. Therefore, such relations can be obtained as follows:

$$\begin{cases} \dot{\tilde{x}}_1 = -\alpha_1 \tilde{x}_1 + \tilde{x}_2 - k_1 |\tilde{x}_1|^{1/2} \operatorname{sgn}(\tilde{x}_1) \\ \dot{\tilde{x}}_2 \in [-F_0, F_0] - \alpha_2 \tilde{x}_1 - k_2 \operatorname{sgn}(\tilde{x}_1) \end{cases} \tag{9}$$

$$\ddot{\tilde{x}}_1 = -\alpha_1 \dot{\tilde{x}}_1 + \dot{\tilde{x}}_2 - \frac{1}{2} k_1 \dot{\tilde{x}}_1 / |\tilde{x}_1|^{1/2} \tag{10}$$

and further

$$\ddot{\tilde{x}}_1 \in [-F_0, F_0] - \alpha_2 \tilde{x}_1 - \left(\alpha_1 \dot{\tilde{x}}_1 + \frac{1}{2} k_1 \dot{\tilde{x}}_1 / |\tilde{x}_1|^{1/2} + k_2 \operatorname{sgn}(\tilde{x}_1) \right) \tag{11}$$

A graph of (11) can be drawn partially for the region $\left[0, \tilde{x}_{1\mathrm{M}}\right]$ as in Fig. 2 shows. Set the initial conditions, $\tilde{x}_1 = 0, x_2 = \dot{\tilde{x}}_1, \hat{x}_2 = 0$, thus $\tilde{x}_2 = x_2$. If the initial value of x_2 is positive, the trajectory will enter into right half-plane. Otherwise it will enter into the left half-plane, and in this article the former condition is discussed. When the trajectory goes in the first quadrant it is confined between $\tilde{x}_1 = 0$, $\dot{\tilde{x}}_1 = 0$ and curve I $\ddot{\tilde{x}}_{1\max} = -(k_2 - F_0)$, let $\left(x_{1\mathrm{M}}, 0\right)$ indicate intersection point of $\dot{\tilde{x}}_1 = 0$ and $\ddot{\tilde{x}}_{1\max} = -(k_2 - F_0)$, $\left(0, \dot{\tilde{x}}_{1_0}\right)$ indicate intersection point of $\tilde{x}_1 = 0$ and $\ddot{\tilde{x}}_{1\max} = -(k_2 - F_0)$, it is easy to get $\dot{\tilde{x}}_{1_0}^2 = 2(k_2 - F_0)\tilde{x}_{1\mathrm{M}}$ by integral calculation. Therefore, the following inequality can be seen.

$$\ddot{\tilde{x}}_1 \leq F_0 - \alpha_2 \tilde{x}_1 - k_2 \operatorname{sgn}(\tilde{x}_1) - \alpha_1 \dot{\tilde{x}}_1 - \frac{1}{2} k_1 \dot{\tilde{x}}_1 / |\tilde{x}_1|^{1/2} < 0 \tag{12}$$

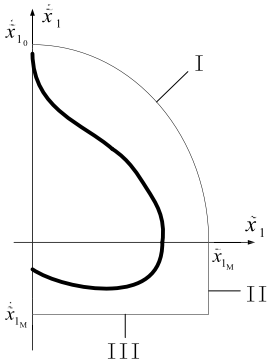

FIGURE 2. Sketch map of majorant trajectory for the observer.

When the trajectory moves toward $\dot{\tilde{x}}_1 = 0$ it can be described by the following equation.

$$\dot{\tilde{x}}_1^2 = 2(k_2 - F_0)\left(\tilde{x}_{1\mathrm{M}} - \tilde{x}_1\right) \tag{13}$$

Then it transits through $\dot{\tilde{x}}_1 = 0$, and enters the forth quadrant and moves towards $\tilde{x}_1 = 0$. If $\ddot{\tilde{x}}_1 = 0$, $\dot{\tilde{x}}_1$ reaches the minimum value as (15) by solving (14).

$$\ddot{\tilde{x}}_1 = F\left(x_1, x_2, \hat{x}_2\right) - \alpha_2 \tilde{x}_1 - \left(\alpha_1 \dot{\tilde{x}}_1 + \frac{1}{2} k_1 \dot{\tilde{x}}_1 / |\tilde{x}_1|^{1/2} + k_2 \right) = 0 \tag{14}$$

$$\begin{aligned} \dot{\tilde{x}}_{1\min} &= 2|\tilde{x}_1|^{1/2} / \left(2\alpha_1 |\tilde{x}_1|^{1/2} + k_1\right) \\ &\quad \times \left[F\left(x_1, x_2, \hat{x}_2\right) - k_2 - \alpha_2 \tilde{x}_1\right] \\ &> -2/k_1 \tilde{x}_{1\mathrm{M}}^{1/2} \left(F_0 + k_2 + \alpha_2 \tilde{x}_{1\mathrm{M}}\right) \end{aligned} \tag{15}$$

Therefore, the trajectory in the fourth quadrant is confined between $\tilde{x}_1 = 0$, $\dot{\tilde{x}}_1 = 0$, $\tilde{x}_1 = \tilde{x}_{1\mathrm{M}}$ (line II) and $\dot{\tilde{x}}_1 = -\left(2\tilde{x}_{1\mathrm{M}}^{1/2}/k_1\right)\left(F_0 + k_2 + \alpha_2 \tilde{x}_{1\mathrm{M}}\right)$ (line III). Given the condition (8) and $\dot{\tilde{x}}_{1_0}^2 = 2(k_2 - F_0)\tilde{x}_{1\mathrm{M}}$, it is easy to derive the conclusion as (16).

$$\begin{aligned} &\left|\dot{\tilde{x}}_{1\mathrm{M}}\right| \Big/ \left|\dot{\tilde{x}}_{1_0}\right| \\ &< \frac{2}{k_1} \tilde{x}_{1\mathrm{M}}^{1/2} \left(F_0 + k_2 + \alpha_2 \tilde{x}_{1\mathrm{M}}\right) \Big/ \left[2(k_2 - F_0)\tilde{x}_{1\mathrm{M}}\right]^{1/2} \\ &< (1-p)\left(F_0 + k_2 + \alpha_2 \tilde{x}_{1\mathrm{M}}\right) \Big/ (k_2 + F_0 + \Lambda)(1+p) \\ &\leq (1-p)/(1+p) < 1 \end{aligned} \tag{16}$$

It can be observed that the point of intersection between the trajectory and $\tilde{x}_1 = 0$ is getting closer and closer to $\tilde{x}_1 = \dot{\tilde{x}}_1 = \tilde{x}_2 = 0$. The theorem 1 is proven.

Theorem 2: The estimation errors $(\tilde{x}_1, \tilde{x}_2)$ can be driven to $(0, 0)$ in a finite time.

Proof: Consider the dynamics of $\tilde{x}_2$ to prove the convergence in a finite time. From the (4), it is easy to get $\tilde{x}_2 = \dot{\tilde{x}}_1$ at the moment $\tilde{x}_1 = 0$ and (17).

$$\begin{aligned} \dot{\tilde{x}}_2 &= -\alpha_2 \tilde{x}_1 + F\left(x_1, x_2, \hat{x}_2\right) - k_2 \operatorname{sgn}(\tilde{x}_1) \\ &= \begin{cases} -\alpha_2 \tilde{x}_1 + F\left(x_1, x_2, \hat{x}_2\right) - k_2 & \tilde{x}_1 > 0 \\ -\alpha_2 \tilde{x}_1 + F\left(x_1, x_2, \hat{x}_2\right) + k_2 & \tilde{x}_1 < 0 \end{cases} \end{aligned} \tag{17}$$

In the axis $\tilde{x}_1 = 0$ it can be observed that:

$$0 < k_2 - F_0 \leq \left|\dot{\tilde{x}}_2\right| \leq k_2 + F_0 \tag{18}$$

Let t_i indicate one time interval between successive intersection points of the trajectory and $\tilde{x}_1 = 0$, integrate (18) over a small neighborhood of its origin, thus

$$(k_2 - F_0)\, t_i \leq \left|\dot{\tilde{x}}_{1_i}\right| \tag{19}$$

and the total convergence time is

$$T = \sum_{i=0}^{\infty} t_i \leq \sum_{i=0}^{\infty} \left|\dot{\tilde{x}}_{1_i}\right| / (k_2 - F) \tag{20}$$

Therefore, the total convergence time is limited because of the decreasing $\left|\dot{\tilde{x}}_{1_i}\right|$ as derived in previous text, therefore, Theorem 2 is proven.

Theorem 3: The proposed observer is stable.

Proof: Consider the Lyapunov function

$$L(\tilde{x}_1) = \frac{1}{2}\tilde{x}_1^2 > 0 \tag{21}$$

and of which derivative is

$$\begin{aligned} \frac{\partial}{\partial t}\left(\frac{1}{2}\tilde{x}_1^2\right) &= e\dot{e} = \tilde{x}_1 \dot{\tilde{x}}_1 \\ &= \tilde{x}_1 \left[-\alpha_1 \tilde{x}_1 + \tilde{x}_2 - k_1 |\tilde{x}_1|^{1/2} \operatorname{sgn}(\tilde{x}_1)\right] \end{aligned} \tag{22}$$

If k_1 meet the requirement of expressed as (23), $L(\tilde{x}_1) \cdot \dot{L}(\tilde{x}_1) < 0$ can be realized and the observer is stable.

When the estimation errors $(\tilde{x}_1, \tilde{x}_2)$ small neighborhood around the origin point (0, 0), considering the (24) according to the infinitesimals of the same order theorem, $\exists k_1 > \mathrm{r}$, $\mathrm{r} \in R^+$, it makes $L(\tilde{x}_1) \cdot \dot{L}(\tilde{x}_1) < 0$.

$$k_1 > \begin{cases} -\alpha_1 |\tilde{x}_1|^{(1/2)} + \tilde{x}_2 / |\tilde{x}_1|^{(1/2)} & \tilde{x}_1 > 0 \\ -\alpha_1 |\tilde{x}_1|^{(1/2)} - \tilde{x}_2 / |\tilde{x}_1|^{(1/2)} & \tilde{x}_1 < 0 \end{cases} \tag{23}$$

$$\lim_{\tilde{x}_1 \to 0, \tilde{x}_2 \to 0} \tilde{x}_2 / |\tilde{x}_1|^{(1/2)} = 0 \tag{24}$$

Remark 4: By introducing the system damping, attraction of error trajectory is enhanced.

Consider the system in (4), in the sliding patch $\dot{\tilde{x}}_1 = 0$, there exist relations as (25).

$$\begin{aligned} \tilde{x}_2 &\le k_1 |\tilde{x}_1|^{1/2} + \alpha_1 \tilde{x}_1 \quad \text{if } \tilde{x}_1 > 0 \\ \tilde{x}_2 &\ge -k_1 |\tilde{x}_1|^{1/2} + \alpha_1 \tilde{x}_1 \quad \text{if } \tilde{x}_1 < 0 \end{aligned} \tag{25}$$

As illustrated in Fig. 3, by introducing the system damping $\alpha_1 \tilde{x}_1$, region of direction attraction is extended, so that trajectory is attracted toward (0, 0) earlier.

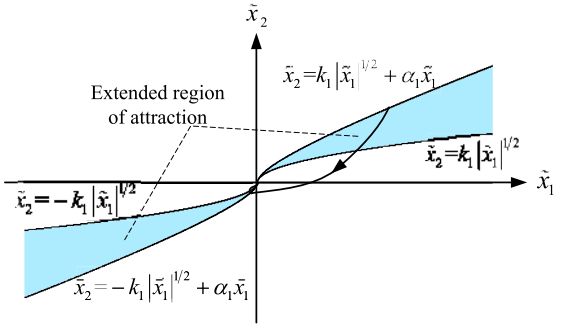

FIGURE 3. Effect of damping on reachability.

IV. OBSERVER PERFORMANCE

In this part, ordinary sliding mode observer, super-twisting sliding mode observer and the proposed accelerated adaptive super-twisting sliding mode observer are selected for comparison in the following figures. To test and compare performance of the three different kinds of observers, selection of corresponding parameters are identical. Let $k_1 = k_2 = 1$, $\alpha_1 = \alpha_2 = 1$, $\lambda_1 = \lambda_2 = 1$, $\mu_1 = \mu_2 = 1$ and the initial value of $\left(\tilde{x}_1, \dot{\tilde{x}}_1\right)$ is supposed to be (10, 10), and they are calculated for the same duration with identical sample time.

It can be observed in the following figures, the conventional sliding mode observer in Fig. 4 takes the longest time to converge the estimation errors to 0 because of the longest spiral trajectory and when the errors are getting close to (0, 0) chattering occurs intensely. The super-twisting sliding mode observer in Fig. 5 performs much better, time consumed for estimation errors convergence is reduced significantly and much less chattering hinders the rate of convergence. The

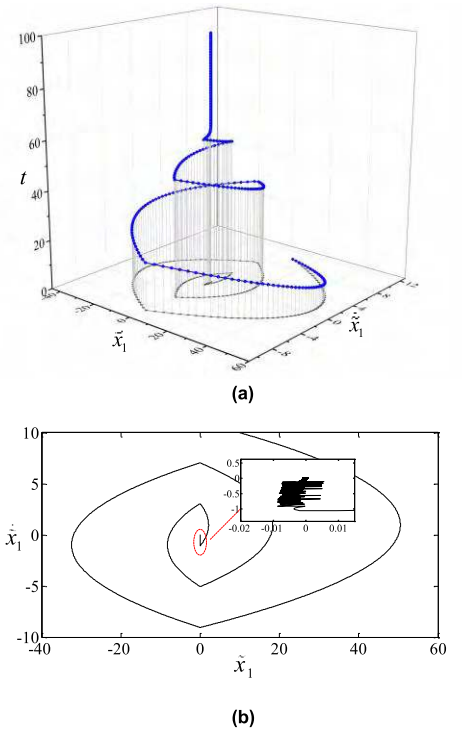

FIGURE 4. Estimation error convergence of ordinary sliding mode observer. (a) 3-D view. (b) Planar graph of upward view.

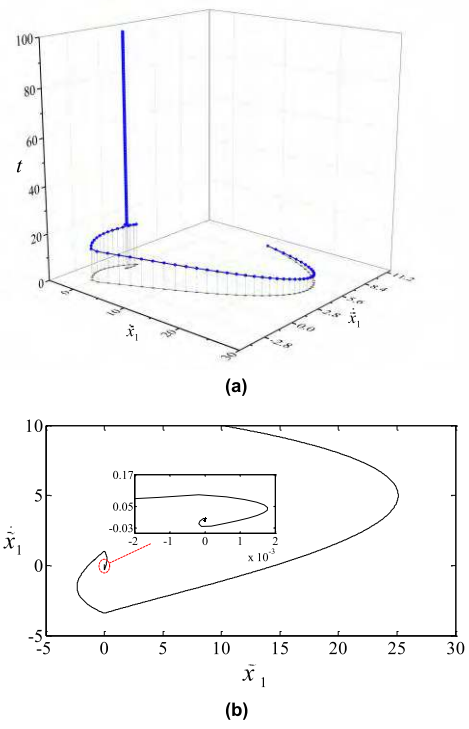

FIGURE 5. Estimation error convergence of super-twisting sliding mode observer. (a) 3-D view. (b) Planar graph of upward view.

proposed accelerated adaptive super-twisting sliding mode observer in Fig. 6 performs the best, the trajectory achieves (0, 0) almost directly, so that the rate of estimation errors

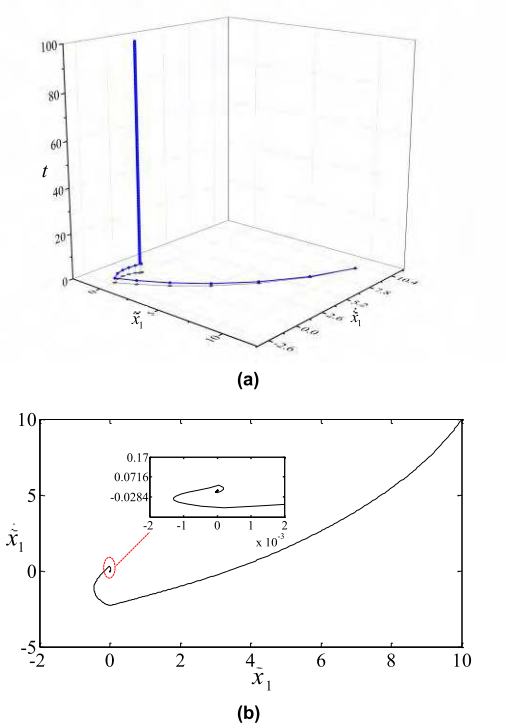

FIGURE 6. Estimation error convergence of accelerated adaptive super-twisting sliding mode observer. (a) 3-D view. (b) Planar graph of upward view.

convergence is accelerated effectively. From the partially enlarged view it can be seen that both STW and AASTW do not bring obvious chattering when the estimation errors get close to the origin. In fact, if the view is further enlarged, the chattering of AASTW is less than that of STW, readers can observe it independently.

V. EXAMPLE

In order to compare and demonstrate performance of the proposed sliding mode observer, the example in reference [27] is considered. It is a pendulum system with Coulomb friction and external perturbation. It is considered a typical nonlinear system that is often selected to test the performance of novel control algorithms [28]. This part is focused on designing a velocity observer for the system and the mathematical model of pendulum is set in (26).

$$\ddot{\theta} = \tau/J - g\sin\theta/L - V_s\dot{\theta}/J - P_s\mathrm{sgn}\left(\dot{\theta}\right)/J + v \quad (26)$$

with the values $M = 1.1$, $g = 9.815$, $L = 0.9$, $J = ML^2$, $V_s = 0.18$, $P_s = 0.45$, v is external disturbance which is also identical to [27], it is simulated as $v = 0.5\sin(2t) + 0.5\cos(5t)$ and the same bounded control signal is used as (27).

$$\tau = -30\mathrm{sgn}\left(\theta - \theta_d\right) - 15\mathrm{sgn}\left(\dot{\theta} - \dot{\theta}_d\right) \quad (27)$$

where $\theta_d = \sin t$, $\dot{\theta}_d = \cos t$, they are the expected signals. In the system, θ is measurable signal, $\dot{\theta}$ is the variable to be estimated. Set $x_1 = \theta$, $x_2 = \dot{\theta}$, the system can be written in

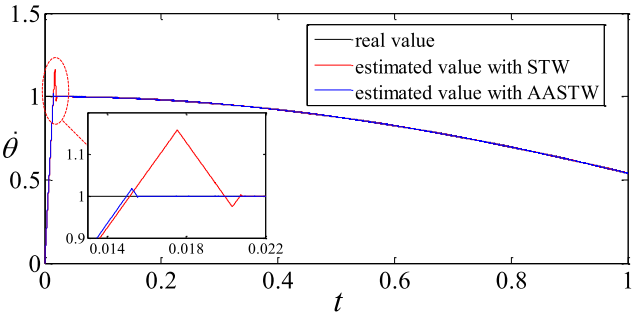

FIGURE 7. Real and estimated velocity.

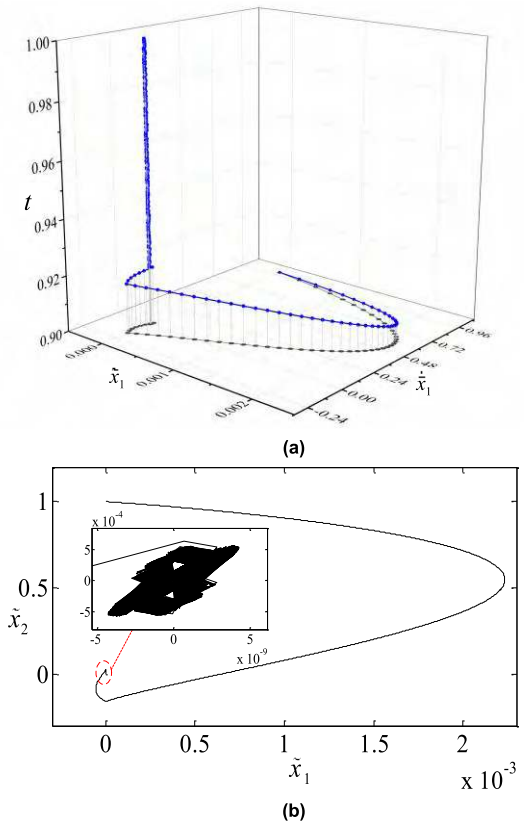

FIGURE 8. Estimation error of velocity with super-twisting sliding mode observer. (a) 3-D view. (b) Planar graph of upward view.

the following form:

$$\begin{cases} \dot{x}_1 = x_2 \\ \dot{x}_2 = \tau/J - g\sin x_1/L - V_s x_2/J - P_s\mathrm{sgn}\left(x_2\right)/J + v \end{cases} \quad (28)$$

The velocity observer based on the proposed accelerated adaptive super-twisting sliding mode algorithm has the form as (29).

$$\begin{cases} \dot{\hat{x}}_1 = \alpha_1\left(x_1 - \hat{x}_1\right) + \hat{x}_2 + k_1\left|x_1 - \hat{x}_1\right|^{1/2}\mathrm{sgn}\left(x_1 - \hat{x}_1\right) \\ \dot{\hat{x}}_2 = \alpha_2\left(x_1 - \hat{x}_1\right) + \tau/J - g\sin x_1/L - V\hat{x}_2/J \\ \qquad + k_2\mathrm{sgn}\left(x_1 - \hat{x}_1\right) \end{cases} \quad (29)$$

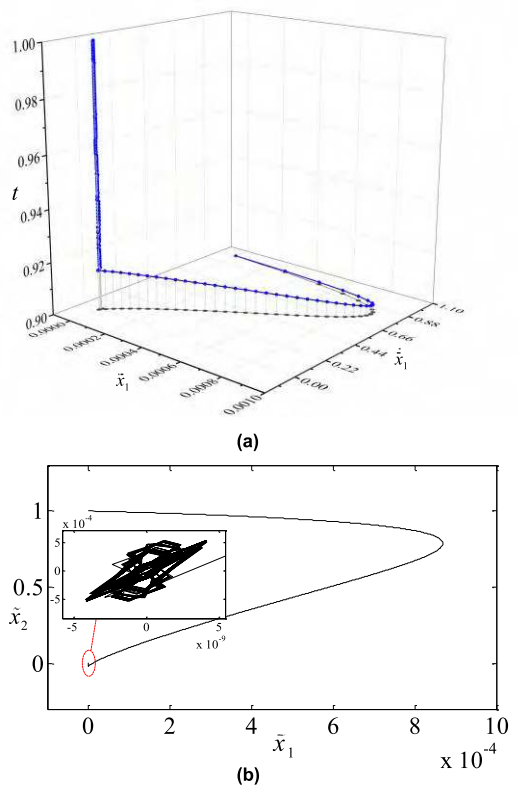

FIGURE 9. Estimation error of velocity with accelerated adaptive super-twisting sliding mode observer. (a) 3-D view. (b) Planar graph of upward view.

θ varies in a compact set of the interval from 0 to 2π, this is a bounded input bounded state stable system, where $\alpha_1 = 500$, $\alpha_2 = 500$, k_1 and k_2 are assigned as follows:

$$\dot{k}_1 = \begin{cases} 12\text{sgn}\left(\left|x_1 - \hat{x}_1\right| - 0.00001\right) & \text{if } k_1 > 6 \\ 0 & \text{if } k_1 \leq 6 \end{cases}$$

$$\dot{k}_2 = \begin{cases} 66\text{sgn}\left(\left|x_1 - \hat{x}_1\right| - 0.00001\right) & \text{if } k_2 > 50 \\ 0 & \text{if } k_2 \leq 50 \end{cases}$$

Initial values of both x_1 and $\hat{x}_1$ are set to 0, initial values of x_2 and $\hat{x}_2$ are set to 1 and 0, respectively, and initial values of k_1 and k_2 are set to 12 and 66, respectively. The solver type is fixed-step with sample time 0.00001s.

Fig. 7 shows performance of the proposed observer by comparing with some other typical sliding mode observers, it can be observed that the estimated velocity converges toward the real values, the super-twisting sliding mode observer proposed by Davila *et al.* [27] performs quite well, however, the main defect, overshoot still exists. It has been reduced further after being accelerated by the proposed algorithm, and with the proposed algorithm it takes the shortest time to converge.

Fig. 8. and Fig. 9. show the trajectories of normal super-twisting sliding mode observer and proposed accelerated adaptive super-twisting sliding mode observer, respectively. From the order of magnitude it is obvious that trajectory of the proposed AASTW observer is the shortest one to achieve (0, 0) target. Chattering is much less than that of the normal super-twisting sliding mode observer.

VI. CONCLUSION AND FUTURE WORK

This article presents a kind of sliding mode observer known as accelerated adaptive super-twisting sliding mode observer. It can satisfactorily attenuate chattering issues and accelerate the rate of convergence for estimation errors by introducing ''system damping''. Mathematical proofs are carried out to ensure the convergence of the proposed observer in a finite time interval. Compared to some typical conventional sliding mode observers and from the pendulum example, the proposed observer performs better without precisely knowing the boundary of uncertainty and disturbance.

Methods to reduce the number of parameters to be selected subjectively or avoid experience-depend work to the largest extent possible, so as to improve the AASTW are future work. This will make it smarter and more accurate.

REFERENCES

[1] S. Yin, H. Gao, J. Qiu, and O. Kaynak, ''Descriptor reduced-order sliding mode observers design for switched systems with sensor and actuator faults,'' *Automatica*, vol. 76, pp. 282–292, Feb. 2017.

[2] Y. Kao, J. Xie, L. Zhang, and H. R. Karimi, ''A sliding mode approach to robust stabilisation of Markovian jump linear time-delay systems with generally incomplete transition rates,'' *Nonlinear Anal., Hybrid Syst.*, vol. 17, pp. 70–80, Aug. 2015.

[3] S. Biricik and H. Komurcugil, ''Optimized sliding mode control to maximize existence region for single-phase dynamic voltage restorers,'' *IEEE Trans. Ind. Informat.*, vol. 12, no. 4, pp. 1486–1497, Aug. 2016.

[4] N. Wang, J. Y. Yu, and W. Y. Lin, ''Positioning control for a linear actuator with nonlinear friction and input saturation using output-feedback control,'' *Complexity*, vol. 21, no. S2, pp. 191–200, Jun. 2016.

[5] J. Liu, S. Vazquez, L. Wu, A. Marque, H. Gao, and L. G. Franquelo, ''Extended state observer-based sliding-mode control for three-phase power converters,'' *IEEE Trans. Ind. Electron.*, vol. 64, no. 1, pp. 22–31, Jan. 2017.

[6] Y. Qin, Z. Wang, C. Xiang, E. Hashemi, A. Khajepour, and Y. Huang, ''Speed independent road classification strategy based on vehicle response: Theory and experimental validation,'' *Mech. Syst. Signal Process.*, vol. 117, pp. 653–666, Feb. 2019.

[7] Y. Qin, C. Xiang, Z. Wang, and M. Dong, ''Road excitation classification for semi-active suspension system based on system response,'' *J. Vib. Control*, vol. 24, no. 13, pp. 2732–2748, Jul. 2018.

[8] Y. Xing, W. He, M. Pecht, and K. L. Tsui, ''State of charge estimation of lithium-ion batteries using the open-circuit voltage at various ambient temperatures,'' *Appl. Energy*, vol. 113, pp. 106–115, Jan. 2014.

[9] X.-S. Si, W. Wang, C.-H. Hu, D.-H. Zhou, and M. G. Pecht, ''Remaining useful life estimation based on a nonlinear diffusion degradation process,'' *IEEE Trans. Rel.*, vol. 61, no. 1, pp. 50–67, Mar. 2012.

[10] J. Liu, C. Wu, Z. Wang, and L. Wu, ''Reliable filter design for sensor networks using type-2 fuzzy framework,'' *IEEE Trans. Ind. Informat.*, vol. 13, no. 4, pp. 1742–1752, Aug. 2017.

[11] Y. Shtessel, M. Taleb, and F. Plestan, ''A novel adaptive-gain supertwisting sliding mode controller: Methodology and application,'' *Automatica*, vol. 48, no. 5, pp. 759–769, 2012.

[12] C. Mu, Y. Tang, and H. He, ''Improved sliding mode design for load frequency control of power system integrated an adaptive learning strategy,'' *IEEE Trans. Ind. Electron.*, vol. 64, no. 8, pp. 6742–6751, Aug. 2017.

[13] A. Levant, ''Homogeneity approach to high-order sliding mode design,'' *Automatica*, vol. 41, no. 5, pp. 823–830, May 2005.

[14] W. A. Apazaperez, L. Fridman, and J. A. Moreno, ''Higher-order sliding-mode observers with scaled dissipative stabilizers,'' *Int. J. Control*, pp. 1–16, Jan. 2017.

[15] A. Pilloni, A. Pisano, and E. Usai, "Observer-based air excess ratio control of a PEM fuel cell system via high-order sliding mode," *IEEE Trans. Ind. Electron.*, vol. 62, no. 8, pp. 5236–5246, Aug. 2015.
[16] L. Xu *et al.*, "Nonlinear observation of internal states of fuel cell cathode utilizing a high-order sliding-mode algorithm," *J. Power Sources*, vol. 356, pp. 56–71, Jul. 2017.
[17] J. J. Rath, K. C. Veluvolu, M. Defoort, and Y. C. Soh, "Higher-order sliding mode observer for estimation of tyre friction in ground vehicles," *IET Control Theory Appl.*, vol. 8, no. 6, pp. 399–408, 2014.
[18] J. A. Moreno and M. Osorio, "A Lyapunov approach to second-order sliding mode controllers and observers," in *Proc. 47th IEEE Conf. Decis. Control*, Dec. 2008, pp. 2856–2861.
[19] E. Guzmán and J. A. Moreno, "Super-twisting observer for second-order systems with time-varying coefficient," *IET Control Theory Appl.*, vol. 9, no. 4, pp. 553–562, Apr. 2015.
[20] A. Levant, "Sliding order and sliding accuracy in sliding mode control," *Int. J. Control*, vol. 58, no. 6, pp. 1247–1263, Dec. 1993.
[21] Y. Dvir and A. Levant, "Accelerated twisting algorithm," *IEEE Trans. Autom. Control*, vol. 60, no. 10, pp. 2803–2807, Oct. 2015.
[22] A. Karthikeyan and K. Rajagopal, "Chaos control in fractional order smart grid with adaptive sliding mode control and genetically optimized PID control and its FPGA implementation," *Complexity*, vol. 2017, Apr. 2017, Art. no. 3815146.
[23] S. Laghrouche, J. Liu, F. S. Ahmed, M. Harmouche, and M. Wack, "Adaptive second-order sliding mode observer-based fault reconstruction for PEM fuel cell air-feed system," *IEEE Trans. Control Syst. Technol.*, vol. 23, no. 3, pp. 1098–1109, May 2015.
[24] T. Gonzalez, J. A. Moreno, and L. Fridman, "Variable gain super-twisting sliding mode control," *IEEE Trans. Autom. Control*, vol. 57, no. 8, pp. 2100–2105, Aug. 2012.
[25] C. L. Baratieri and H. Pinheiro, "New variable gain super-twisting sliding mode observer for sensorless vector control of nonsinusoidal back-EMF PMSM," *Control Eng. Pract.*, vol. 52, pp. 59–69, Jul. 2016.
[26] J. J. E. Slotine, J. K. Hedrick, and E. A. Misawa, "On sliding observers for nonlinear systems," in *Proc. Amer. Control Conf.*, Jun. 1986, pp. 1794–1800.
[27] J. Davila, L. M. Fridman, and A. Levant, "Second-order sliding-mode observer for mechanical systems," *IEEE Trans. Autom. Control*, vol. 50, no. 11, pp. 1785–1789, Nov. 2005.
[28] M. Jouini, S. Dhahri, and A. Sellami, "Design of robust supertwisting algorithm based second-order sliding mode controller for nonlinear systems with both matched and unmatched uncertainty," *Complexity*, vol. 2017, Dec. 2017, Art. no. 1972921.

CHENG LIN was born in Wuhan, Hubei, China, in 1968. He received the B.S. and M.S. degrees from the Wuhan University of Technology and the Ph.D. degree from the Beijing Institute of Technology. He is currently a Professor and a Doctoral Supervisor with the Beijing Institute of Technology. His research focuses on dynamic control, structural optimization, and lightweight for electric vehicle.

SHENGXIONG SUN was born in Shenyang, Liaoning, China, in 1989. He received the B.S. degree in vehicle engineering from the Shenyang Aerospace University, Shenyang, in 2012, and the M.S. degree in vehicle from Northeastern University, Shenyang, China, in 2014. He is currently pursuing the Ph.D. degree with the Beijing Institute of Technology, Beijing, China, and the University of Technology Sydney, Sydney, NSW, Australia. His research focuses on nonlinear dynamic control for electric vehicle (EV), especially torsional vibration control for EV powertrains and nonlinear control algorithm.

PAUL WALKER was born in Sydney, NSW, Australia, in 1981. He received the B.E. and Ph.D. degrees in mechanical engineering from the University of Technology Sydney (UTS) in 2007 and 2011, respectively. Since 2011, he has been a Research Associate with the School of Electrical, Mechanical and Mechatronic Systems, UTS, where he is currently a Chancellor's Post-Doctoral Research Fellow. His research interests include the development of novel power splitting transmissions for hybrid electric vehicles, multi-speed transmission dynamics and control, and novel hybrid and electric vehicle topologies and their control.

NONG ZHANG received the Ph.D. degree from The University of Tokyo in 1989. He worked at several universities in China, Japan, USA, and Australia. He joined the University of Technology Sydney in 1995. Since 2009, he has been a Professor of mechanical engineering with the School of Electrical, Mechanical and Mechatronic Systems, University of Technology Sydney. He focused on fundamental research on mechanical vibration, multi-body system dynamics, and its applications to complex machines and vehicular systems. He developed advanced models and numerical schemes for simulating gear shift in powertrains with AT, MT, and CVTs and for dynamic analysis of vehicles fitted with advanced suspensions.